Improved Li-ion Transport by DME Chelation in a Novel Ionic Liquid Based Hybrid Electrolyte for Li-S Battery Application

Urbi Pal,[a] Gaetan M. A. Girard,[a] Luke A. O'Dell,[a] Binayak Roy [a, b,] Xiaoen Wang,[a] Michel Armand,[a ,c] Douglas R. MacFarlane,[d] Patrick C. Howlett,[a] Maria Forsyth[a]*

[a] Institute for Frontier Materials (IFM), Deakin University, Burwood, Victoria 3125, Australia.

[b] Department of Energy Science & Engineering, Indian Institute of Technology, Bombay, 400076, India.

[c] CIC EnergiGUNE, Parque Tecnológico de Álava, 48, 01510 Miñano, Álava, Spain.

[d] School of Chemistry, Monash University, Clayton 3800, Victoria, Australia.

ABSTRACT: Current Li-S battery technology has yet to reach the promise of high capacity and suffers rapid capacity fade due in large part to the dissolution and diffusion of polysulphide intermediates. The electrolyte plays a significant role here as well as in stabilising the Li metal anode electrochemistry. In this work a novel hybrid electrolyte system is investigated based on varying composition of *N*-methyl, *N*-propyl pyrrolidinium bisfluorosulfonimide (C_3mpyrFSI) ionic liquid and *1,2* dimethoxy ether (DME) at the saturated concentration of LiFSI salt, demonstrating a most favourable performance for an 80:20 IL: DME composition (by weight). This electrolyte presented higher ionic conductivity and diffusivity, while simultaneously improving the electrochemical behaviour of Li metal plating and stripping. The ionic interactions among different species of the electrolyte have been studied by NMR spin lattice relaxation time (T_1) measurements, which indicated that Li-DME is likely to form chelation compounds, thereby breaking down the larger ionic aggregates and resulting in smaller solvation shell and higher ionic mobility. An *ex-situ* polysulphide dissolution study indicated that the hybrid electrolyte is also efficient in eliminating polysulphide dissolution. Therefore, due to its ability to suppress polysulphide dissolution and enhance Li transport properties, while minimising the volatile organic solvent component, the hybrid electrolyte system is an excellent candidate to further explore for future Li-S systems.

1. Introduction:

The proliferation of portable electronic devices and the development of new emerging electronic technologies (*e.g.* drones or artificial intelligence systems) require high energy density storage devices. Beyond the conventional Li-ion battery, the most promising device is the Lithium Sulphur (Li-S) system due to its high theoretical specific capacity of 1672 mAh/g and high theoretical specific energy density of 2600 Wh/kg.[1] Despite the high energy density, the implementation of Li-S technology in large-scale applications remains a challenge due to several hurdles related to the unique features of Li-S chemistry. The major two drawbacks of Li-S battery are (1) the dissolution and diffusion of the lithium polysulphide intermediate products (Li_2S_n, $8 \leq n \leq 4$) that are generated at the sulphur electrode during reduction of sulphur (S_8), resulting in loss of active materials with rapid capacity fading,[2] and (2) the formation of dendrites at the Li metal anode leading to poor cyclic performance and internal short circuit,[3] compromising safety of these devices. The Li-S battery performance and the extent of polysulphide dissolution has been observed to depend significantly on electrolyte composition among other parameters. The archetypical electrolyte for Li-S cell, in the most recent studies, has reported to be a binary ether mixture (v/v) of *1,3* dioxolane (DOL) and *1,2* dimethoxy ethane (DME), doped with 1 M lithium bis(trifluoromethanesulfonyl)imide (LiTFSI) salt.[4] However, a few studies suggest that a high salt concentration in the electrolyte helps to retard the polysulphide diffusion rate as a result of a "salting out" due to common ion effect.[5] Along this line, Suo *et al*. systematically studied the effect of LiTFSI salt from 1 to 7 M in DME/DOL solvent and introduced the concept of 'Solvent in salt electrolyte' (SolIS) when the Li salt concentration was above 4 M. Interestingly they showed excellent performance over 100 cycles with the capacity retention of *ca.* 100%, along with complete suppression of polysulphide dissolution, and a dendrite free Li morphology.[6] Despite all

the above advantages, these ethers based electrolytes are still highly flammable and volatile, thus, possesses a serious fire hazard. Additionally, it has been shown that DOL can undergo a cleavage leading to the formation of alkoxy moieties at the reactive lithium metal[7-9] which is not desirable in the long term.

From the perspective of chemical, thermal and electrochemical stability, room temperature ionic liquids (RTILs), are now receiving more attention as viable electrolytes. Since the last decade, there has been an increasing number of reports of ILs in battery applications due to their low flammability, high ionic conductivity and good thermal and electrochemical stability compared to organic solvents.[10-12] In the context of Li-S applications, various ILs have been used. In a recent study by Park *et al*., emphasis has been given to understand how the IL anions affect polysulphide reactivity and they proposed that the solubility of polysulphides is governed by the donor ability of the IL anion. In that study, TFSI, FSI, OTf, BETI, BF_4 anions were studied and they concluded that the polysulphide dissolution was hampered in the ILs which having fluorosulfonyl amide type anions due to their weak donor ability to the Li cation of polysulphide (Li_2S_n).[13] Among various cations, the pyrrolidinium cations (*e.g.* as in C_3mpyrFSI IL) showed an impressive first discharge capacity of 1000 mAh/g. However, Shin *et al*., reported C_4mpyrFSI and tetraglyme (G4) as a mixed solvent and noted that the resistance was lower compared to the neat IL.[14] Later, Wang *et al.*, used 1 M LiTFSI in PiP13TFSI and DME mixture replacing DOL and successfully reported very high cycling performance at 1C rate with nearly 100% efficiency and suppressed overcharge.[15] Hence, the concept of a mixed electrolyte has initiated a new area of electrolyte research, demanding further investigations to understand the individual and cumulative effects of the IL, salt and organic solvent as 'hybrid' electrolyte components in the Li-S batteries.

Besides preventing the polysulphide dissolution, it is necessary to protect the Li metal anode surface for long term cycling. Very recent research focuses on the stabilization of the Li metal anode in the presence of various ionic liquid electrolyte. A systematic study consisting of a small phosphonium cation based ionic liquid, tri (methyl isobutyl) phosphonium FSI (P_{111i4}FSI), with varying LiFSI salt concentration from 0.8-3.2 mol/kg (0.6-3.4 M respectively)[16-17] and suggested an increase in Li salt concentration led to a decrease in the ionic conductivity while the high salt concentration facilitated Li metal plating due to the availability of a large amount of Li^+ in the electrolyte and higher Li^+ transport number. Further, Yoon *et al*. investigated C_3mpyrFSI ionic liquid with various LiFSI concentrations (0-3.2mol/kg) and they also reported the influence on ionic conductivity on electrolyte composition and showed high Li^+ transference number along with very stable electrochemical behaviour and a stable SEI layer at the Li metal anode.[18-19] Therefore, irrespective of the electrolyte composition, Li-salt concentration plays a crucial role, from stabilising the Li metal anode to suppressing the polysulphide dissolution, both required for high performance of a Li-S battery. However, the design of highly concentrated electrolyte systems is largely dependent on the thermodynamic stability of Li-salt solvates.[20]

Given the individual advantages of ionic liquids, ether organic solvents and the effects of high salt concentrations, in this work we will discuss novel electrolyte systems based on a mixture of an RTIL (C_3mpyrFSI) and an ether (DME) in the presence of high LiFSI salt concentration. We investigate the effect of electrolyte compositions on the physical and chemical properties associated with these electrolytes including their ability to inhibit polysulphide dissolution. An extensive study in ionic conductivity, PFG NMR along with spin-lattice relaxation NMR (T_1) have been carried out to elucidate the mechanism of Li transport within the electrolyte medium.

2. Experimental:

2.1. Materials: Ionic liquid *N*-propyl-*N*-methylpyrrolidinium bis(fluorosulfonyl)imide (C_3mpyrFSI, Figure 1a) was purchased from Solvionic (France) with 99.5% purity, Li-salt of bis(fluorosulfonyl)imide (LiFSI) was ordered from Nippon Shokubai (Japan) with 99.5% purity and used without further purification. *1,2* dimethoxy ethane (DME, Figure 1c) was purchased from Sigma-Aldrich with 99.9% purity (anhydrous) and all the materials were kept at Argon filled glove box for further preparation of materials.

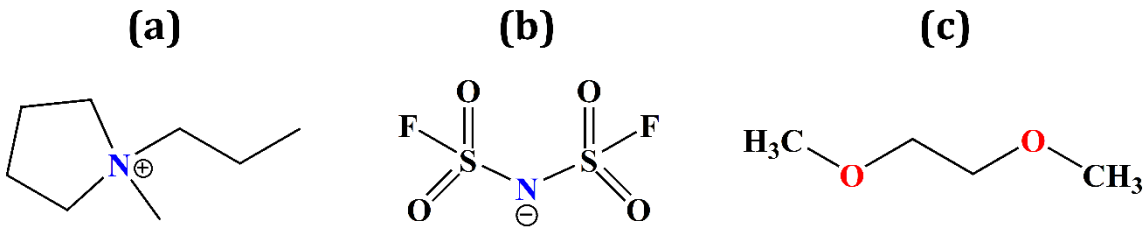

Figure 1. Chemical structures of (a)C_3mpyr$^+$, (b)FSI$^-$, (c)DME

2.2. Sample Preparation: The ionic liquid was dried under vacuum on a Schlenk-line at 50˚C for 48 hours before using. The dried IL and DME were mixed in various weight ratios starting from 100:0, 80:20, 60:40, 50:50, 40:60, 20:80, 0:100 (IL: DME) and LiFSI salt was dissolved in these mixed solvents to prepare saturated solutions. The highest concentration was determined by dissolving the salt at 50˚C for 24 hours whilst stirring, and then allowing the electrolytes to settle at room temperature until the undissolved lithium salt decanted out for each of the mixtures. The weight of the mixtures (with their corresponding LiFSI concentrations) was measured and concentrations are expressed as molal (m) LiFSI concentration (mol/kg). All materials were subsequently kept in an Argon filled glove box before further characterization. The Table 1 below summarises the LiFSI molality concentrations and corresponding molar ratio of species present in

each composition studied so far. Interestingly, even though the molality increases significantly with increasing DME, the relative number of moles of Li^+ ions remains relatively constant against the other species in the mixture.

Table 1. LiFSI saturated molality and molar ratio of ionic species in the hybrid electrolytes

Composition	m (LiFSI) mol.kg^{-1}	Li^+	FSI^-	C_3mpyr^+	DME
100IL	3.2	0.25	0.50	0.25	0
80IL20DME	6.2	0.28	0.40	0.12	0.20
60IL40DME	8.0	0.28	0.35	0.07	0.30
50IL50DME	9.2	0.28	0.33	0.05	0.33
40IL60DME	10.4	0.28	0.32	0.04	0.36
20IL80DME	12.6	0.29	0.30	0.01	0.40
100DME	13.6	0.28	0.28	0	0.44

The moisture content of the electrolyte was measured by using a model 831 Karl Fisher Coulometer (Metrohm) and Hydranal Coulomat AG was used as titrant. The moisture content of ionic liquid based hybrid electrolytes was maintained <20ppm. The standard error for the water content measurement was about ± 1%.

2.3. Materials Characterisation:

The conductivity of the electrolytes was determined by AC impedance spectroscopy using MTZ frequency response analyser using frequencies between 0.1Hz to 1MHz and amplitude of 100 mV.

A custom-built dip-cell was used where two platinum wire electrodes were kept at a fixed distance. Measurements were taken over a temperature range of -30 ˚C to 60 ˚C and the temperature below 10 ˚C was obtained using liquid nitrogen. The cell constant was determined using standard 0.01M KCl solution at 25˚C and the resistance was calculated from the value of x-axis intercept of the Nyquist plot.

The viscosity was measured using an Anton Paar viscometer coupled with a density meter where the mode for viscosity was Lovis 2000ME and density was DMA5000. A 10mm long capillary with a diameter of 2.5mm was filled with electrolyte and 'rolling ball' method was applied with a constant tilting angle for free falling of the metal ball to measure viscosity. An 'Oscillating U-tube principle' method was used to measure the density of these ionic liquid based electrolytes. Measurements were performed between 20˚C and 60˚C with 10˚C intervals.

A Perkin Elmer Spectrum 400 was used to record FTIR spectra. A diamond crystal ATR was used in an Argon atmosphere and a drop of each electrolyte was placed on the crystal to record the spectra at room temperature. 16 scans from 4000 cm^{-1} to 500 cm^{-1} were accumulated per sample.

A Mettler Toledo DSC1 instrument was used to determine the phase behaviour of the ionic liquid-based electrolytes, using a heating rate of 10 ˚C/min and cooling rate of 20 ˚C/min. The temperature range of the analysis was chosen from -150˚C to 60˚C with a sample loading of approximately 10mg. Cyclohexane was analysed as a reference to calibrate the instrument.

Pulsed-field gradient stimulated echo (PFG-STE) diffusion measurements for ^{1}H, ^{7}Li and ^{19}F were performed with a Bruker Avance III 7.05 T spectrometer equipped with a 5 mm Diff50 gradient probe using the gradient pulse time (δ = 2 ms) and the diffusion time (Δ = 25 ms), following the method described by Bayley *et al.*[21] The ^{1}H and ^{19}F nuclei were used to determine

the diffusion coefficients for the pyrrolidinium cation and FSI anion respectively. ^{1}H PFG NMR was also used for measuring diffusion for the DME molecules while ^{7}Li NMR gave the diffusion of the lithium ion species. The chemical shifts of ^{7}Li are reported relative to a 2M LiCl solution. Samples were filled to a height of 50 mm in 5 mm NMR tube in an Argon filled glove box and sealed with Teflon tape and a cap. All the measurements were carried out at 20 ˚C.

The spin-lattice relaxation (T_1) measurements were carried out using the same hardware as the PFG experiments to probe the dynamics of the cation and anion of IL as well as the Li cation and DME molecule. The measurements of various nuclei of ^{1}H, ^{19}F, and ^{7}Li were possible by tuning the probe for the resonance frequencies at 300, 282 and 117 MHz, respectively with temperatures between 20 and 80 °C. All T_1 measurements were performed using a saturation recovery sequence. The T_1 values were obtained from fitting the recovery in signal to an exponential function within the TopSpin software. The resulting variable temperature T_1 data was fitted to Bloembergen-Purcell-Pound (BPP) theory[22] following the method described previously.[23]

Cyclic voltammetry (CVs) experiments were performed using a Biologic SP200 potentiostat. CVs were obtained using a conventional three electrode arrangement. A 1.5mm diameter nickel electrode was used as working electrode to investigate Li plating and stripping. CV measurements were carried out in the presence of a counter electrode of Platinum wire (APS, 99.95%) and reference electrode consisted of silver wire immersed in a solution of ionic liquid containing 5mM silver triflate (AgOTf) separated by a glass frit. The potentials were corrected versus ferrocene after each experiment. All the measurements were carried out at room temperature and at 20mV/sec scan rate.

3. Results and discussion:

3.1. Physical properties and ionic diffusivities: For the following discussion, we introduce a hybrid electrolyte consisting of an ionic liquid, C_3mpyrFSI and an ether, DME with varying ratios (w/w) in the presence of LiFSI salt. The LiFSI salt solubility (or saturation point) as a function of DME ratio is shown in Figure 2a. The graph indicates that the introduction of DME into the ionic liquid facilitates LiFSI salt solubility. Previously, Yoon *et al.*, studied the gradual addition of LiFSI in neat C_3mpyrFSI ionic liquid and they found the LiFSI solubility was 3.2 mol/kg;[18] this is confirmed by our findings here for the 100:0 (IL: DME) composition. LiFSI solubility in the hybrid electrolyte is observed to be higher with increase in DME content. In the presence of 20% DME (80:20) in the hybrid electrolyte, the LiFSI salt solubility increases to 6.2 mol/kg, almost double than that in neat ionic liquid system (100:0). The increasing trend in salt solubility is followed in the rest of the electrolyte compositions (i.e. 60:40, 50:50, 40:60 etc). Interestingly, in this systematic study such a high amount of LiFSI solute is dissolved without any phase separation (Figure S1). Thus, this successive increase in the LiFSI solubility indicates that the addition of DME concomitantly increases the available Li solvation sites within the electrolyte.

Ionic conductivity (Figure 2b) was recorded over a temperature range of -30˚C to 60˚C. A gradual decrease in ionic conductivity is noted for all the electrolytes at the higher temperature range (60 to 20˚C) whereas a rapid fall in magnitude is observed at low temperature region (10 to -30˚C), as is typically expected for Vogel-Tammann-Fulcher (VTF) behaviour. We observe that for the saturated 100IL, the ionic conductivity is $8.3*10^{-4}$ S/cm at 20 ˚C while introduction of just 20% DME (80IL20DME) increases the conductivity over the entire temperature range with a value of $1.1*10^{-3}$ S/cm at 20˚C, despite the higher LiFSI concentration in the latter case. With increasing DME and concomitant increase in LiFSI, the conductivity does decrease a little in the hybrid systems, in particular at lower temperatures, consistent with a more viscous system and an

increasing glass transition temperature (T_g). This is seen clearly in the DSC traces (Figure S1) which reveals a distinct T_g for each hybrid electrolyte. For 100IL, the T_g value appears at -72.9˚C whereas for 80IL20DME, the T_g value is -69˚C and for 50IL50DME, the T_g is -63.7˚C. These hybrid electrolytes showed comparable glass transition temperature with the electrolyte with 7M LiTFSI in DOL/DME (-77.3 ˚C) [6] ensuring good low temperature performances.

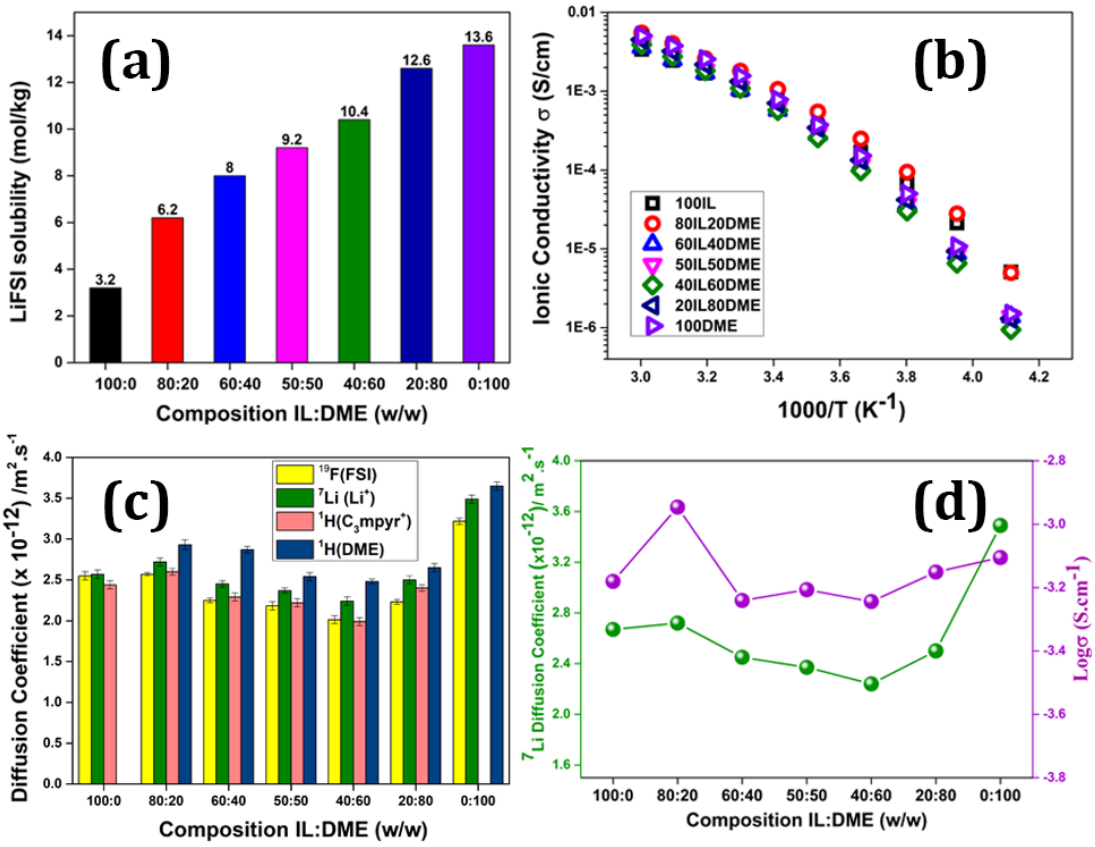

Figure 2. a) LiFSI salt solubility of various ionic liquid based hybrid electrolytes; b) Temperature dependent ionic conductivity, c) Diffusion coefficient values of ionic species of saturated ionic liquid based hybrid electrolytes, and d) Comparison of ionic conductivity and ^{7}Li diffusion coefficients of saturated ionic liquid based hybrid electrolytes.

The ionic conductivity is dependent on both the viscosity and mobility of ionic species. In the temperature dependent viscosity study, as all the compositions are saturated with LiFSI salt, the corresponding viscosity values show similar magnitudes for different compositions of hybrid

electrolytes (Figure S2a). Also, we did not observe any significant change in density for the electrolytes over the temperature range studied (Figure S2b). To further determine the diffusivity of ionic species, PFG NMR measurements for ^{7}Li, ^{1}H and ^{19}F nuclei were measured to study the diffusion of Li^{+}, C_3mpyr^{+} cation and DME, as well as the FSI^{-} anion respectively and the diffusion coefficient values of corresponding ionic species are plotted against electrolyte composition in Figure 2c. For the saturated 100IL system, the FSI^{-} anion moves faster than the C_3mpyr^{+} cation whilst the Li^{+} shows comparative diffusivity to the FSI^{-} anion, implying that the diffusion of these two species is coupled and likely results from an aggregated structure.[18] However, for all other compositions, DME (blue) diffuses faster than the other species present in the system. Interestingly Li^{+} is the second most diffusive species, following to DME whilst the FSI^{-} and C_3mpyr^{+} ions diffusion coefficients seem more closely correlated, at least in the intermediate compositions. This phenomenon indicates that the addition of DME changes the environment of Li^{+} present in the system, dominating its coordination and thus transport.

A comparative graph is plotted in Figure 2d to focus on the trend in behaviour of Li^{+} diffusion and the effect of ionic conductivity with respect to the compositions. In both the cases, saturated 80IL20DME (80:20) composition shows an improved ionic conductivity and a slight increase in the Li^{+} diffusion coefficient. However, the highest Li^{+} diffusivity was obtained for saturated 100DME (0:100 composition) among the rest of the compositions. DME is a linear ether with sp^3 carbons and with two oxygen centres. Thus, to explain this behaviour, one may imagine that Li^{+} may be present in a tunnel like orientation (gauche-trans-gauche) provided by the oxygen from the ether for the saturated 100DME electrolyte, which facilitates the movement of Li. However, in mixed IL and DME systems, the transport mechanism of Li^{+} is complex due to a competition among the DME, FSI^{-} anion and C_3mpyr^{+} cation. Hence it is necessary to focus on the interactions

between species present in the ionic liquid based hybrid electrolytes to understand the influence of various ions and their local environments.

3.2. Interactions with ionic species:

FTIR: In order to rationalise the increased conductivity and interaction between Li^+, C_3mpyr^+ and FSI^- in saturated hybrid electrolytes, FTIR spectra of all solutions were recorded (Figure 3). The peaks are assigned based on reported 0.5 mol/kg LiTFSI in C_3mpyrFSI by Hardwick *et al.* [24] and are listed in Table S1. In Figure 3a, the C-O-C stretching vibrations are plotted for all the saturated hybrid electrolytes. The C-O-C stretching vibration for pure DME (without LiFSI salt) is observed at 1110 cm^{-1} (Figure S3). Interestingly, LiFSI addition leads to a lowering of the stretching vibration to 1078 cm^{-1} for all the hybrid electrolytes where DME is present as co-solvent. The decrease in Li—O interaction frequency reveals that the strong interaction between Li^+ and the oxygen from C-O-C, weakens in turn the C-O-C bond.

In Figure 3b, the S-N-S stretching vibrations from FSI^- anion is shown for different saturated electrolytes. Previously, the neat IL, C_3mpyrFSI (without LiFSI salt) showed S-N-S stretching frequency at 730cm^{-1} which shifted to higher number (747 cm^{-1}) when LiFSI salt was added into the IL.[18] Fuji *et al.*, suggested that the shift in higher frequency of S-N-S stretching implied a change in coordination between FSI^- and Li^+.[25] Further, they suggested that the FSI^- anion converted from *trans* to *cis* conformer in the presence of increasing amount of LiFSI salt. However, in the present study, as we introduce more DME to the electrolyte, we detected the S-N-S stretching frequency at 747 cm^{-1} with an additional shoulder peak at 774 cm^{-1}. The appearance of the shoulder peak may lead to the existence of both *cis* and *trans* conformer of FSI^- anion in the electrolyte systems.

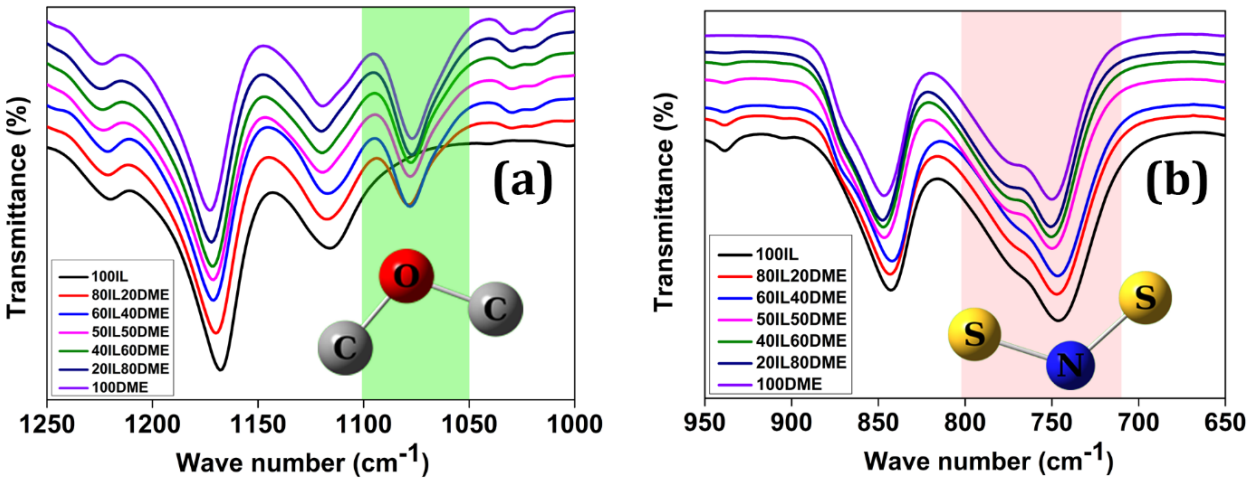

Figure 3. FTIR transmittance a) From 1250 to 1000 cm^{-1} and b) 950 to 650 cm^{-1}. Note that, this figure is plotted in stack mode to represent a comparative study for various saturated electrolyte systems where each component contains their corresponding amount of LiFSI salt

Chemical shift analysis: To understand the effect of DME addition on Li speciation and coordination with other ionic components in the electrolyte system, the NMR spectra (1D) of ^{7}Li was studied. The ^{7}Li NMR spectra (Figure 4a) shows a sharp shift to higher frequency from 100IL to 80IL20DME and the same trend is observed for the other compositions. The relative peak shift is plotted against composition in Figure 4b. The subsequent change in chemical shift suggests that the Li^{+} cation environment is changing with increasing DME concentration. To explain this phenomenon, it can be noted that DME has a higher donor number (DN 18.6)[3] than the FSI^{-} anion (DN 5.5)[26], and will therefore interact more strongly with the Li ions. Hence, the ^{7}Li nuclei become increasingly de-shielded due to the proximity of the electronegative oxygen atoms present in the DME molecules (Li—O) leading to a change in the coordination of Li as well as its transportation. Hence this interaction justifies the behaviour of Li^{+} diffusivity observed in the diffusion study (Figure 2c) where Li^{+} shows very similar diffusivity to the DME.

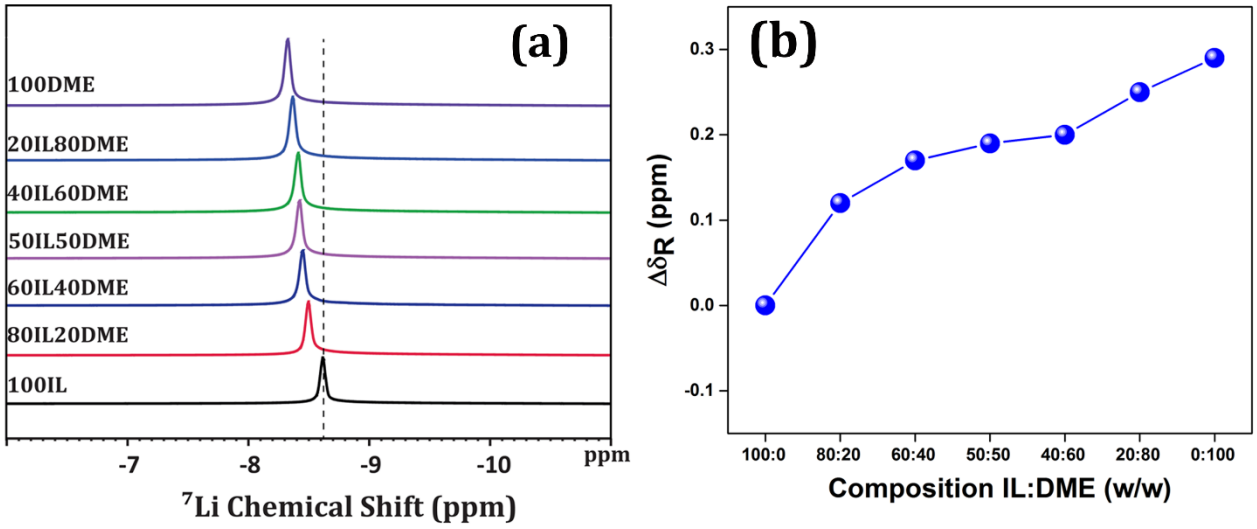

Figure 4. a) Chemical shift of ^{7}Li peak for different saturated hybrid electrolytes, b) Relative comparison of ^{7}Li peak shift due to interaction

Spin-lattice (T_1) relaxation measurements:

To probe the changes in chemical environment and fast-timescale dynamics of the ionic species as a function of temperature, NMR spin−lattice (T_1) relaxation measurements have been performed. T_1 values are plotted in Figure 5 and the curves are fitted to the expressions based on BPP theory.[22] From the previous sections, we note that among these compositions, 80IL20DME shows improved transport properties thus, in the following sections the focus will be on a few selected systems. As the use of the highly flammable solvent (DME) should be minimised, we focus on the 100IL, 80IL20DME, however for a comparison of the effect between the IL dominant phase and DME dominant phase, the 20IL80DME is also examined.

The temperature dependent ^{1}H T_1 relaxation times are shown in Figures 5a and 5b. The present compositions contain two types of ^{1}H nuclei, one from the C_3mpyr^+ cation and another from DME. To probe the molecular dynamics of the C_3mpyr^+ cation, the T_1 value was measured using the

resolved peak from the ring proton nuclei marked as H6 (Figure S4). The relatively rigid nature of the pyrrolidinium ring means that the relaxation of this proton will be caused primarily by the rotational dynamics of the cation. On the other hand, the ^{1}H signal from the DME (labelled separately as H2 in Figure S4) was also fitted in a similar way, represented in Figure 5b. The resulting parameters are listed in Table 2. For the C_3mpyr^+ cation, the ^{1}H T_1 minimum is shifted to a higher temperature with the increase in DME ratio. This can be explained by the slower rotational dynamics of the C_3mpyr^+ cation with increasing DME content which is consistent with the increasing T_g and lower diffusion.[23]

Table 2. The BPP fitting parameters for ^{1}H T_1 relaxation measurements

^{1}H	**Composition**	**E_a (kJ mol^{-1})**	**τ_c (300 K, s^{-1})**
C_3mpyr	100IL	16.5± 2.0	(1.6±0.1) ×10^{-10}
	80IL20DME	19.0± 1.5	(2.1±0.2) ×10^{-10}
	20IL80DME	21.0± 1.5	(3.2±0.1) ×10^{-10}
DME	80IL20DME	11.6± 1.8	(2.2±0.1) ×10^{-10}
	20IL80DME	9.0± 1.5	(3.4±0.4) ×10^{-10}

The ^{1}H nuclei of DME also shows a decrease in molecular dynamics as the DME content increases, reflected by the higher correlation time (τ_c), (*i.e.* the average time taken for the molecule to rotate by 1 radian) and higher activation energy (E_a) for this rotational motion. The activation energy for the cation rotation is higher due to its larger size. The higher mobility of DME was also reflected in the diffusion measurements above. The increasing correlation times for both the cation and DME imply stronger associations with their neighbouring species as the DME content increases.

The ^{19}F T_1 measurements also shows a shift in T_1 minima to higher temperatures suggesting hindered dynamics for the FSI^- anion (Figure 5d). The hindered rotational dynamics and the comparable diffusion coefficient of both the C_3mpyr^+ cation and FSI^- anion suggest a strong interaction between these two species, probably electrostatic in nature, which occurs to a greater extent when more DME is present (and consequently more FSI^- due to higher saturated LiFSI concentration). For the 100IL composition, the activation energies for the cation, anion and Li are similar and reveal comparable diffusion rates (Figure 2d). However, increasing the DME content changes the behaviour, where the E_a for the rotational dynamics of both anion and cation increases due to the presence of more FSI^- anions into the system.

Table 3. The BPP fitting parameters of ^{19}F T_1 relaxation measurements

^{19}F	**E_a (kJ mol^{-1})**	**τ_c (300 K, s^{-1})**
100IL	17.6±1.8	(4.2±0.5) ×10^{-10}
80IL20DME	21.8±1.0	(5.2±0.3) ×10^{-10}
20IL80DME	24.3±1.5	(6.3±0.3) ×10^{-10}

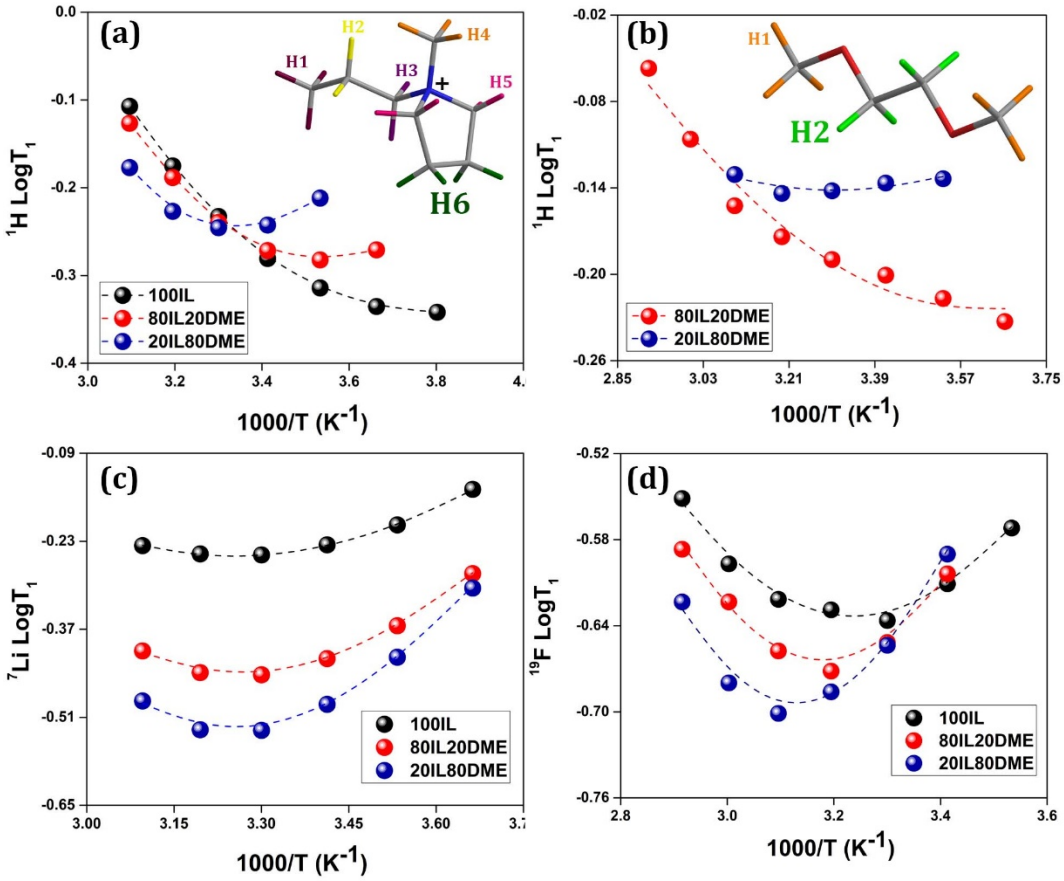

Figure 5. T_1 relaxation time measurements of a) ^{1}H nuclei of the IL cation, b) ^{1}H nuclei of the DME, c) ^{7}Li nuclei, d)^{19}F nuclei of FSI^- anion of the selected electrolytes in the presence of their corresponding LiFSI salt.

Notably, the ^{7}Li T_1 minimum does not shift in temperature significantly with higher DME content, although the magnitude of the T_1 decreases considerably which indicates a change in the environment around the Li (Figure 5c). As the LiFSI concentration is increasing with the DME addition, a shift to high temperature would also have been expected here, as with the other nuclei, and from a previous study of concentrated Li salt systems due to formation of larger clusters.[18, 23] However, clearly this behaviour is not observed here. From the solubility plot of composition (Figure 2a), the addition of DME facilitates the LiFSI solubility by creating more coordination options for the Li^+ ion. Two oxygen centres of one DME molecule effectively provide a solvation

shell for Li, forming a chelate structure. Thus, the DME coordination provides an alternative mechanism for the Li^+ relaxation process. Since ^7Li is a quadrupolar nucleus, the changing coordination environment may change the quadrupolar coupling constant and also the dipolar contribution to the relaxation process is now ^1H-^7Li rather than ^{19}F-^7Li. This would then account for the significant decrease in the magnitude of the T_1 minimum. The NMR results here therefore suggest that DME addition drags the Li^+ ion from its anionic environment, which results in stronger FSI anion-pyrrolidinium cationic interactions which would decrease their rotational dynamics. The enhanced C_3mpyr and FSI interactions do not impede the ionic conductivity of Li, as the Li-DME coordination appears to provide a higher mobility. As a result, the ionic conductivity value for the electrolyte is not significantly compromised, and in fact increases in the 80IL20DME system.

Table 4. The BPP fitting parameters of ^7Li T_1 relaxation measurements

^{7}**Li**	E_a **(kJ mol^{-1})**	τ_c **(300 K, s^{-1})**
100IL	16.2±1.8	(9.8±1.8) ×10^{-10}
80IL20DME	21.3±1.0	(9.8±1.8) ×10^{-10}
20IL80DME	25.1±1.8	(10.6±1.8) ×10^{-10}

3.3. Electrochemical study:

Cyclic voltammetry (CV) is used to evaluate the Li plating (negative scan) and stripping (positive scan) behaviour of the ionic liquid based hybrid electrolytes. In this study, the electrolytes are subjected to a reduced potential window of -4V vs Ag/AgOTf and the corresponding stripping behaviours are noted at room temperature. From Figure 6, all the compositions show very stable cycling performance up to 5 cycles. Comparison between 100IL and 80IL20DME, showed higher

current density in case of the latter composition during Li stripping process. It is noted that further increase in DME ratio reduced the Li stripping current density for 20IL80DME. The comparison of peak current trend clearly shows a more facile process in case of 80IL20DME which correlates with the diffusion measurements presented above.

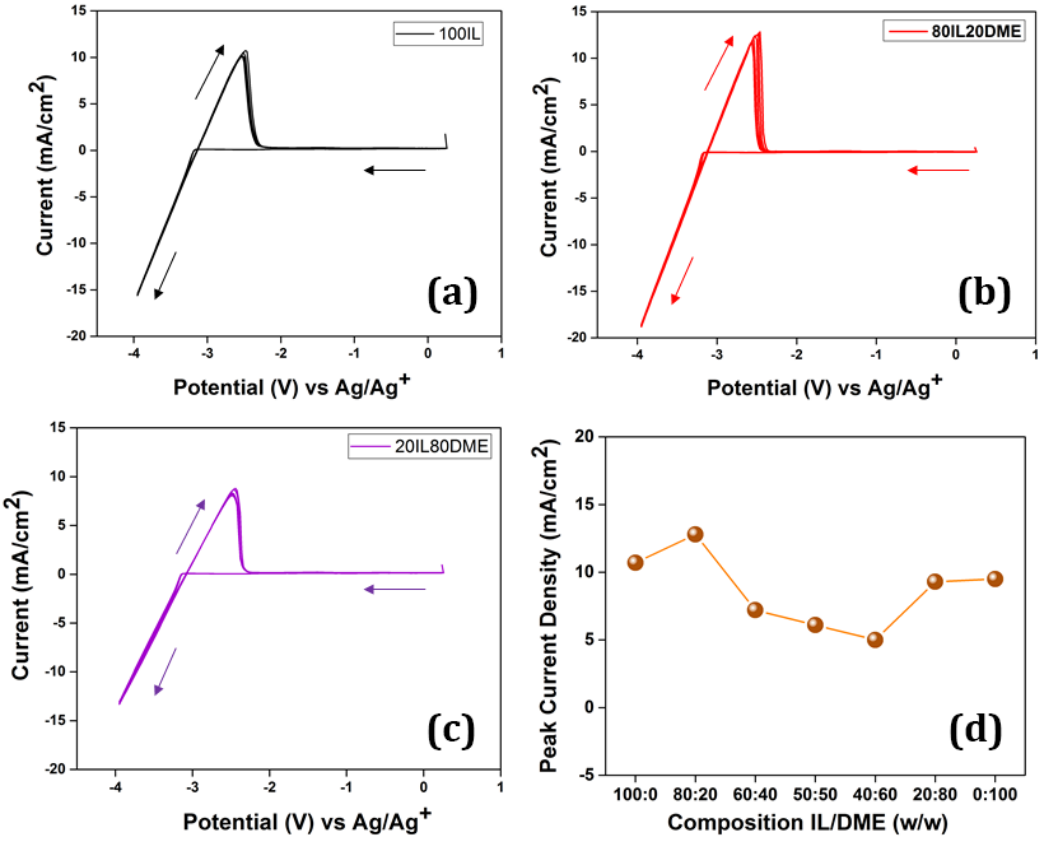

Figure 6. Cyclic voltammograms of a) 100IL, b) 80IL20DME, c)20IL80DME and d) Comparison of peak current density of Li plating stripping at different compositions

3.4. Polysulphide Dissolution Test:

An *ex-situ* polysulphide dissolution test has been carried out following the method reported by Suo *et. al*.[6] In this study, Electrolyte-1 is the conventional electrolyte used in Li-S battery which consists of 1M LiTFSI in DME/DOL (v/v) and Electrolyte-2 is 80IL20DME composition. The systematic comparison of several compositions indicated that 80IL20DME is the most promising candidate amongst the compositions studied which showed impressive performance with respect to ionic conductivity, diffusivity and electrochemical Li plating-stripping behaviour. Hence this composition has been chosen to compare with the conventional liquid electrolyte (Electrolyte-1) with respect to the dissolution of polysulphide.

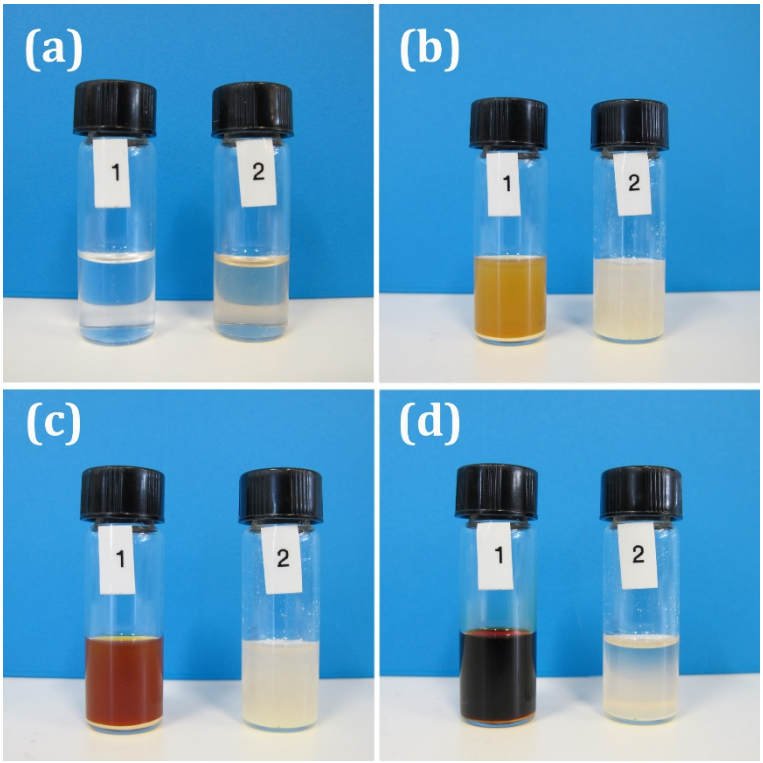

Figure 7. Colour changes of the two samples containing same amount of Li_2S_8 were recorded by digital camera with respect to time; a) Before addition, b) After 30 mins, c) After 2 hours, d) After 1 week.

In Figure 7, the gradual change in colour from yellow to dark brown in Electrolyte-1 indicates the dissolution of polysulphides in the electrolyte medium whereas the colour of Electrolye-2 remains unchanged over the same time period. The Electrolyte-2 consists of saturated LiFSI salt in which the polysulphide intermediate is hardly soluble, resulting in a turbid appearance. The initial reduced products of S_8 (Li_2S_n where, $8 \leq n \leq 4$) are known to be highly soluble in typical liquid electrolytes considered for an Li-S battery, whereas here we can establish that in the novel ionic liquid based hybrid electrolyte, the dissolution of polysulphides is completely inhibited.

4. Conclusion:

In the present study, a series of hybrid electrolytes with varying IL and DME compositions were prepared and their physical and electrochemical properties were investigated. We observed an increase in LiFSI salt concentration with increase in DME content due to higher molecular interaction among them. The high solvating nature of DME influenced the LiFSI salt solubility and the higher donor ability also changes the lithium coordination environment exhibiting an improved lithium ionic conductivity and diffusivity. The positive effect on transport properties and lithium ion mobility is observed to be most favourable for the 80IL20DME composition.

The diffusion coefficient is found to be the highest for DME while Li^+ is observed to be the next most diffusive species in the hybrid mixtures. ^{7}Li chemical shift suggests a strong interaction between the Li^+ ion and oxygen centres provided by DME which facilitates the fast transport of Li^+ ion for the hybrid mixtures. Interestingly the NMR relaxation measurements imply a lower activation energy for rotational dynamics of DME while slower dynamics are observed for the C_3mpyr^+ cation and FSI^- anion which likely result from a stronger ionic association where the presence of DME decreases the Li^+/FSI^- interactions.

The hybrid electrolytes show a promising electrochemical behaviour for Li plating and stripping with peak current densities higher than 10mA/cm^2. Furthermore, we have demonstrated the viability of ionic liquid based hybrid electrolytes for potential use in the Li-S battery by showing the lack of solubility of polysulfides. Further work, including galvanostatic charge-discharge, cyclic voltammetry and electrochemical impedance measurements are currently underway.

▪ ASSOCIATED CONTENT

Supporting Information. The following files are available free of charge.

Differential Scanning Calorimetry (DSC) curve, Viscosity and Density measurements, FTIR spectra and list of peaks, ^{1}H NMR spectra.

▪ AUTHOR INFORMATION

Corresponding Author

*Tel: +61392446818

Email: maria.forsyth@deakin.edu.au

▪ NOTES:

The authors declare no competing financial interest.

▪ ACKNOWLEDGMENTS:

This work is financially supported by the Australia-India Strategic Research Fund (AISRF, grant agreement No.48515). Professors Maria Forsyth and Douglas MacFarlane thank the ARC for

their respective Australian Laureate Fellowship (FL110100013 and FL120100019). Deakin University's Advanced Characterisation Facility is acknowledged for use of the NMR facility.

- **REFERENCES:**

1. Ji, X.; Nazar, L. F., Advances in Li-S batteries. *Journal of Materials Chemistry* **2010,** *20* (44), 9821-9826.
2. Sun, Y.; Seh, Z. W.; Li, W.; Yao, H.; Zheng, G.; Cui, Y., In-operando optical imaging of temporal and spatial distribution of polysulfides in lithium-sulfur batteries. *Nano Energy* **2015,** *11*, 579-586.
3. Scheers, J.; Fantini, S.; Johansson, P., A review of electrolytes for lithium–sulphur batteries. *Journal of Power Sources* **2014,** *255*, 204-218.
4. Zhang, S. S., Liquid electrolyte lithium/sulfur battery: Fundamental chemistry, problems, and solutions. *Journal of Power Sources* **2013,** *231* (Supplement C), 153-162.
5. Shin, E. S.; Kim, K.; Oh, S. H.; Cho, W. I., Polysulfide dissolution control: the common ion effect. *Chemical Communications* **2013,** *49* (20), 2004-2006.
6. Suo, L.; Hu, Y.-S.; Li, H.; Armand, M.; Chen, L., A new class of solvent-in-salt electrolyte for high-energy rechargeable metallic lithium batteries. *Nature communications* **2013,** *4*, 1481.
7. Aurbach, D.; Youngman, O.; Dan, P., The electrochemical behavior of 1, 3-dioxolane—LiClO4 solutions—II. Contaminated solutions. *Electrochimica acta* **1990,** *35* (3), 639-655.
8. Aurbach, D.; Youngman, O.; Gofer, Y.; Meitav, A., The electrochemical behaviour of 1, 3-dioxolane—LiClO 4 solutions—I. Uncontaminated solutions. *Electrochimica acta* **1990,** *35* (3), 625-638.
9. Gofer, Y.; Ely, Y. E.; Aurbach, D., Surface chemistry of lithium in 1, 3-dioxolane. *Electrochimica acta* **1992,** *37* (10), 1897-1899.
10. Hallett, J. P.; Welton, T., Room-Temperature Ionic Liquids: Solvents for Synthesis and Catalysis. 2. *Chemical Reviews* **2011,** *111* (5), 3508-3576.
11. Zhang, Z.; Zhou, H.; Yang, L.; Tachibana, K.; Kamijima, K.; Xu, J., Asymmetrical dicationic ionic liquids based on both imidazolium and aliphatic ammonium as potential electrolyte additives applied to lithium secondary batteries. *Electrochimica Acta* **2008,** *53* (14), 4833-4838.
12. Zhang, Z.; Yang, L.; Luo, S.; Tian, M.; Tachibana, K.; Kamijima, K., Ionic liquids based on aliphatic tetraalkylammonium dications and TFSI anion as potential electrolytes. *Journal of Power Sources* **2007,** *167* (1), 217-222.
13. Park, J.-W.; Ueno, K.; Tachikawa, N.; Dokko, K.; Watanabe, M., Ionic liquid electrolytes for lithium–sulfur batteries. *The Journal of Physical Chemistry C* **2013,** *117* (40), 20531-20541.
14. Shin, J. H.; Cairns, E. J., N-Methyl-(n-butyl) pyrrolidinium bis (trifluoromethanesulfonyl) imide-LiTFSI–poly (ethylene glycol) dimethyl ether mixture as a Li/S cell electrolyte. *Journal of Power Sources* **2008,** *177* (2), 537-545.
15. Wang, L.; Byon, H. R., N-Methyl-N-propylpiperidinium bis(trifluoromethanesulfonyl)imide-based organic electrolyte for high performance lithium–sulfur batteries. *Journal of Power Sources* **2013,** *236* (Supplement C), 207-214.
16. Girard, G. M. A.; Hilder, M.; Nucciarone, D.; Whitbread, K.; Zavorine, S.; Moser, M.; Forsyth, M.; MacFarlane, D. R.; Howlett, P. C., Role of Li Concentration and the SEI Layer in Enabling High Performance Li Metal Electrodes Using a Phosphonium Bis(fluorosulfonyl)imide Ionic Liquid. *The Journal of Physical Chemistry C* **2017,** *121* (39), 21087-21095.

17. Girard, G. M. A.; Hilder, M.; Zhu, H.; Nucciarone, D.; Whitbread, K.; Zavorine, S.; Moser, M.; Forsyth, M.; MacFarlane, D. R.; Howlett, P. C., Electrochemical and physicochemical properties of small phosphonium cation ionic liquid electrolytes with high lithium salt content. *Physical Chemistry Chemical Physics* **2015,** *17* (14), 8706-8713.
18. Yoon, H.; Best, A. S.; Forsyth, M.; MacFarlane, D. R.; Howlett, P. C., Physical properties of high Li-ion content N-propyl-N-methylpyrrolidinium bis(fluorosulfonyl)imide based ionic liquid electrolytes. *Physical Chemistry Chemical Physics* **2015,** *17* (6), 4656-4663.
19. Yoon, H.; Howlett, P. C.; Best, A. S.; Forsyth, M.; MacFarlane, D. R., Fast Charge/Discharge of Li Metal Batteries Using an Ionic Liquid Electrolyte. *Journal of The Electrochemical Society* **2013,** *160* (10), A1629-A1637.
20. Yamada, Y.; Yamada, A., Review—Superconcentrated Electrolytes for Lithium Batteries. *Journal of The Electrochemical Society* **2015,** *162* (14), A2406-A2423.
21. Bayley, P. M.; Lane, G. H.; Rocher, N. M.; Clare, B. R.; Best, A. S.; MacFarlane, D. R.; Forsyth, M., Transport properties of ionic liquid electrolytes with organic diluents. *Physical Chemistry Chemical Physics* **2009,** *11* (33), 7202-7208.
22. Bloembergen, N.; Purcell, E.; Pound, R., Principles of nuclear relaxation. *Phys Rev* **1948,** *73*, 679-712.
23. Pope, C. R.; Kar, M.; MacFarlane, D. R.; Armand, M.; Forsyth, M.; O'Dell, L. A., Ion Dynamics in a Mixed-Cation Alkoxy-Ammonium Ionic Liquid Electrolyte for Sodium Device Applications. *ChemPhysChem* **2016,** *17* (20), 3187-3195.
24. Hardwick, L. J.; Saint, J. A.; Lucas, I. T.; Doeff, M. M.; Kostecki, R., FTIR and Raman Study of the Li x Ti y Mn1 − y O2 (y = 0 , 0.11) Cathodes in Methylpropyl Pyrrolidinium Bis(fluoro-sulfonyl)imide, LiTFSI Electrolyte. *Journal of The Electrochemical Society* **2009,** *156* (2), A120-A127.
25. Fujii, K.; Fujimori, T.; Takamuku, T.; Kanzaki, R.; Umebayashi, Y.; Ishiguro, S.-i., Conformational equilibrium of bis (trifluoromethanesulfonyl) imide anion of a room-temperature ionic liquid: Raman spectroscopic study and DFT calculations. *The Journal of Physical Chemistry B* **2006,** *110* (16), 8179-8183.
26. Linert, W.; Camard, A.; Armand, M.; Michot, C., Anions of low Lewis basicity for ionic solid state electrolytes. *Coordination chemistry reviews* **2002,** *226* (1-2), 137-141.